Journal of Optoelectronics and Advanced Materials, Vol. 3, No. 2, June 2001, p. 521 - 524

# VISIBLE LIGHT EMISSION FROM $Cd_{1-X}Mn_XS$ NANOCRYSTALS

V. Ghiordanescu, M. Sima, M. N. Grecu, L. Mihut

National Institute of Materials Physics, PO Box MG-7
76900 Bucharest-Magurele, Romania

The luminescence spectra of some $Cd_{1-x}Mn_xS$ nanocrystals have been measured at room and liquid nitrogen temperature. The $Mn^{2+}$ ions give rise to a broad emission band centered at about 580 nm, between the emission bands of CdS host.

(Received May 8, 2001; accepted June 11, 2001)

*Keywords*: $Cd_{1-x}Mn_xS$ nanocrystals, Optical and EPR spectra

## 1. Introduction

Optical properties of the nanocrystaline semiconductors were extensively studied in the last years. Due to the quantum confinement, the large surface/volume ratio and the high density of the surface states, these materials differ from the bulk crystals. Most
studies were performed on the pure semiconductors [1-5]. To improve emission activity have been performed researches on the doped nanocrystaline semiconductors like ZnS: Mn [6-8] or CdS:Mn [9-11]. The d-electronic states of the $Mn^{2+}$ ions act as the luminescence centers emitting in the green part of the visible spectrum; the efficiency increases by energy transfer from s-p states of the host nanocrystal. On the other side, recent studies [7,8] showed that the emission intensity increases as a result of surface modification, which appears when the nanocrystals are imbedded in an acrylic polymer.

In our paper we report some results of the study concerning the influence of $Mn^{2+}$ion and poly(p-aminobenzoic acid) (PABA) matrix on the optical properties of
$Cd_{1-x}Mn_xS$ nanocrystals.

## 2. Synthesis

$Cd_{1-x}Mn_xS$ nanoparticles were prepared at room temperature by $H_2S$ bubbling into $H_2O$/THF (tetrahydrofuran) (1:4 vol.) solution containing $CdCl_2$ and $MnCl_2$ in different molare ratios; the concentration of the cations, $[Cd^{2+}] + [Mn^{2+}]$ was kept at $10^{-3}$ M. The pH of the solution before treatment with hydrogen sulfide was 8.5. Sodium thioglycollate ($10^{-3}$M), as stabilizing agent was added in this solution. The precipitated nanoparticles were maintained in this medium during 48 h and then separated. To obtain a composite film PABA/$Cd_{0.95}Mn_{0.05}S$ the nanocrystals were redispersed into $H_2O$/THF (9:10 vol.) and were mixed with PABA; the polymer was prepared using the procedure described in [12]. For optical measurements the $Cd_{1-x}Mn_xS$ nanoparticles and the composite were deposited on the quartz glass substrate. The $Cd_{0.95}Mn_{0.05}S$ particles dimension was estimated to be ~10 nm from the micrograph (Fig.1) obtained with a Philips EM 301 electron microscope.

## 3. Results and Discussion

Fig. 2 shows *the absorption spectra* at room temperature (RT) for $Cd_{0.95}Mn_{0.05}S$ (a), $Cd_{0.75}Mn_{0.25}S$ (b) and PABA/$Cd_{0.95}Mn_{0.05}S$ composite film (c). Curves (a) and (b) show a main peak due to CdS, near 400 nm and several weak superimposed structures (Table 1) which can be attributed to $Mn^{2+}$ ions, according to literature data [13-15]; the 405 and 414 nm absorption peaks are due to transitions of excited CdS states [3] . Curve (c) doesn't show these absorption peaks; a nanoparticles' agglomeration process can be produced in composite sample. The assignments of the $Mn^{2+}$ transitions given in Table 1 are in agreement with literature data [13-15].

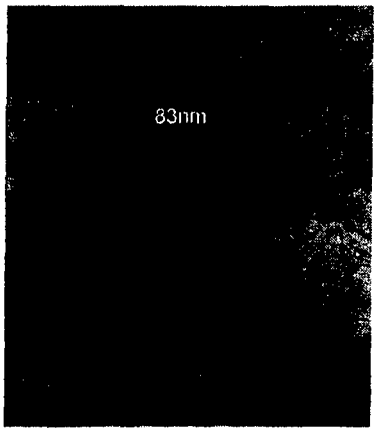


Fig. 1. Transmission electron micrograph of $Cd_{0.95}Mn_{0.05}S$ nanoparticles.

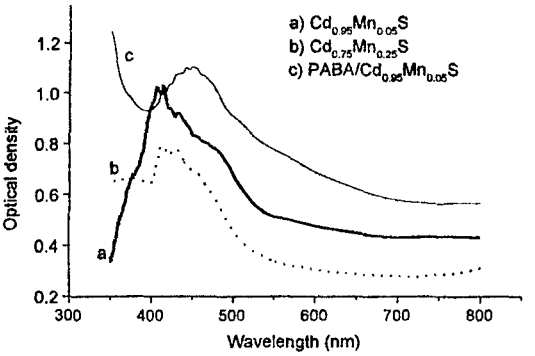


Fig. 2. Absorption spectra of $Cd_{0.95}Mn_{0.05}S$, $Cd_{0.75}Mn_{0.25}S$ nanoparticles and PABA/ $Cd_{0.95}Mn_{0.05}S$ composite film, at RT.

Table 1. The $Mn^{2+}$ absorption and photoluminescence excitation (PLE) maxima for $Cd_{1-x}Mn_xS$ nanoparticles.

| $^1A_6 \rightarrow$ | | $^4T_1(^4G)$ | $^4T_2(^4G)$ | $^4E, ^4A_1(^4G)$ | $^4T_2(^4P)$ | $^4E(^4P)$ | $^4T_2(^4D)$ |
|---|---|---|---|---|---|---|---|
| $Cd_{0.6}Mn_{0.4}S$, crystal [13] | | 510 | 480 | 445 | - | - | - |
| $Zn_{0.95}Mn_{0.05}S$, crystal [14] | | 531 | 498 | 466 | 429 | 389 | - |
| $Zn_{0.94}Mn_{0.6}S$*, film [15] | | 550 | 500 | 465 | 430 | 380 | - |
| $Cd_{0.95}Mn_{0.05}S$, our results | Abs. (Fig.2) | - | 485 | 463 | 430 | 373 | 360 |
| | PLE (Fig.4) | 508 | 490 | 465 | 429 | 373 | 361 |

*estimated from transmission spectrum

*The photoluminescence (PL) spectra* were registered at RT and liquid nitrogen temperature (LNT) using the exciting light from an $Ar^+$ laser ($\lambda$=457.9 nm) and a SPEX double monochromator with EMI 9658 A photomultiplier. The geometry was $90^0$ and the registration by photon counting.
Table 2 presents the positions of the maxima and their intensities observed on the PL spectra (Fig.3). Assuming that the emission spectrum is composed by three Gaussian curves, the maximum centered at 510 nm at LNT is attributed to CdS band to band transition [1]. The red luminescence (652-673 nm) is due to CdS defect states. The emission maximum (576-596 nm) located between CdS bands is attributed to the $Mn^{2+}$ ions ($^4T_1 \rightarrow {}^6A_1$ transition), in accordance with [9-11].
The relative efficiency of manganese PL increases as far as temperature and $Mn^{2+}$ concentration decreases (Table 2).

Table 2. PL intensity (I) and peak position ($\lambda$, nm) of the $Cd_{0.95}Mn_{0.05}S$ (a), $Cd_{0.75}Mn_{0.25}S$ (b) nanoparticles and PABA/ $Cd_{0.95}Mn_{0.05}S$ composite film(c), obtained by deconvoluting the PL spectra.

| | a) | | b) | | c) | |
|---|---|---|---|---|---|---|
| | $\lambda$ | I | $\lambda$ | I | $\lambda$ | I |
| **LNT** | 510 | 1.3 | 518 | 1.6 | 509 | 2.3 |
| | 586 | 22.1 | 596 | 5.9 | 576 | 4.0 |
| | 652 | 10.5 | 673 | 8.9 | 663 | 4.0 |
| **RT** | 539 | 1.0 | 525 | 0.3 | 523 | 0.7 |
| | 579 | 1.2 | 564 | 0.8 | 573 | 2.0 |
| | 659 | 1.2 | 674 | 0.7 | 670 | 1.9 |

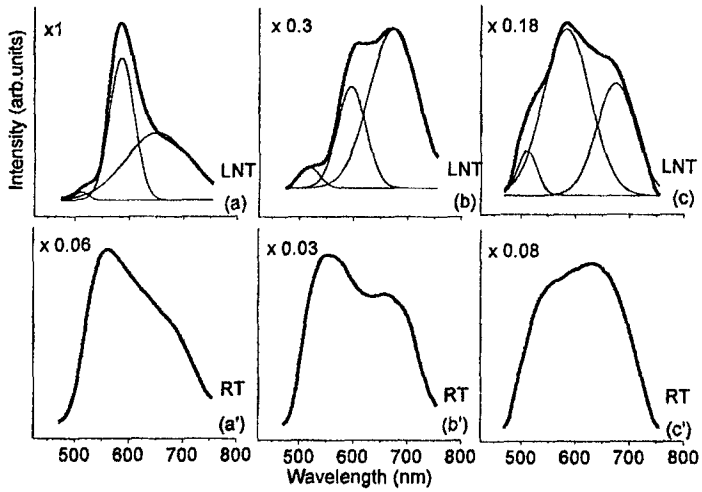


Fig. 3. Photoluminescence spectra of $Cd_{0.95}Mn_{0.05}S$ (a,a'), $Cd_{0.75}Mn_{0.25}S$ (b,b') nanoparticles and PABA/ $Cd_{0.95}Mn_{0.05}S$ (c,c') composite film, at RT and LNT.

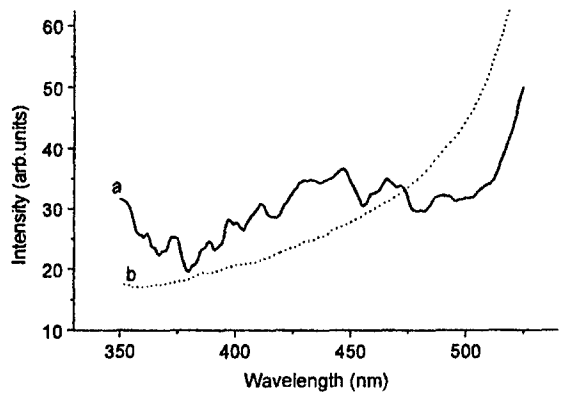


Fig. 4. Photoluminescence excitation spectra of $Cd_{0.95}Mn_{0.05}S$ nanoparticles in the 570 nm (curve a)and 750 nm (curve b) spectral region, at RT.

*The photoluminescence excitation (PLE) spectra* (Fig. 4) were obtained in the 320-550 nm range, using a SPM-2 monochromator with tungsten lamp and EMI 6558 QB photomultiplier. The sample was irradiated in the $45^0$ geometry arrangement using a cut filter and interferential filters, which permit detection at the 570 nm and 750 nm. The data were corrected using a $BaSO_4$ diffuser as reference.

One can observe in the Fig. 4, curve (a) the presence of several weak peaks, which are attributed to the $Mn^{2+}$ absorption [13-15]. The supplementary peaks from 446, 411, 396 and 388 nm can be attributed to CdS host [3]. The CdS luminescence from 510 nm is a result of these absorptions and it is superimposed on the $^1A_6 \rightarrow {}^4T_1$ $Mn^{2+}$ absorption; an energy transfer from CdS host to manganese emitting centers can be produced. The shape of the curve (b) (Fig. 4) registered for the red emission follows filter transmission; the presence of very weak peaks in the 400 nm region confirms that the red emission is due to some defects' states in the gap of CdS.

*X-band EPR spectra* were recorded at room temperature for $Cd_{1-x}Mn_xS$ nanoparticles deposited on quartz plate. In figure 5 are shown broad EPR signals in three samples with different concentrations of manganese ions: 5%, 25%, respectively 5% and dispersed in polymer. Absorption is mainly observed in the region of $g_{eff}$ = 2.01. No resolved hyperfine structure is observed. The broadening of the EPR line width increases with the concentration of manganese ions from 12 mT (in sample with 5% Mn) to 19 mT (for 25% Mn). The sample dispersed in polymer has a narrower line (11 mT). We note that these values are much smaller than those reported in [16]. Besides, the EPR spectra for samples with low concentration of Mn ions are changing in time. In figure 5(a) one can see such a behaviour; the spectrum of two distinct EPR signals observed for fresh samples is drastically

modified after six weeks, the sample being kept at room temperature. Such modifications are associated with an aggregation process of the $Cd_{1-x}Mn_xS$ nanoparticles deposited on quartz glass substrate.

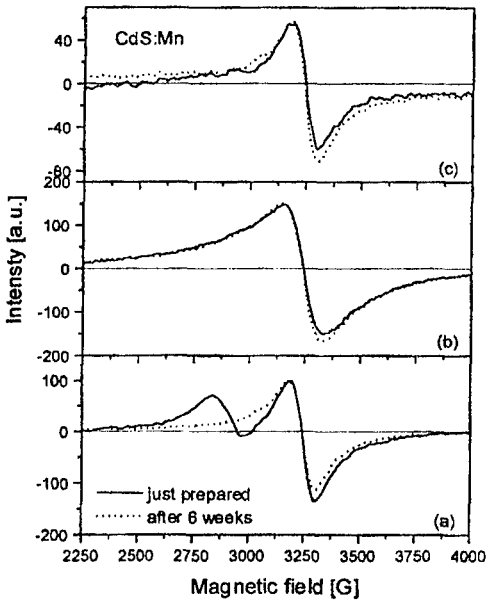


Fig. 5. Room temperature EPR spectra of $Cd_{0.95}Mn_{0.05}S$ (a), $Cd_{0.75}Mn_{0.25}S$ (b) nanoparticles and PABA/ $Cd_{0.95}Mn_{0.05}S$ (c) composite film.

## 4. Conclusions

The absorption spectra of $Cd_{1-x}Mn_xS$ particles show a main absorption due to CdS host and several weak peaks superimposed on it; some of them are attributed to $Mn^{2+}$ ions in accordance with the PLE spectrum of the yellow-green emission.

The PL spectra show three components in the 500-800 nm spectral region. Their intensities at RT are at the same order of magnitude.

Our results show an energy transfer from CdS host to manganese dopant.

EPR and emission spectra confirm two manganese location; they apear due to nonuniform distribution of $Mn^{2+}$ ions inside nanoparticle.

## References

[1] J.J. Ramsden, M. Grätzel, J.Chem.Soc.,Faraday Trans, **1**, 80, 919 (1983).
[2] A.P. Alivisatos, A.L. Harris, N.J. Levinos, M.L. Steigerwald, L.Brus, J.Phys.Chem., **89**, 4001 (1988).
[3] K.K. Nanda, S.N. Sarangi, S. Mohanty, S.N. Sahu, Thin Solid Films, **322**, 21 (1998).
[4] S. Pethkar, R.C. Patil, J.A. Kher, K. Vijayamohanan, Thin Solid Films, **349**, 105 (1999).
[5] T. Nakanishi, B. Ohtani, K. Uosaki, J. Phys. Chem., **102**, 1571 (1998).
[6] R.N. Bhargava, D. Gallagher, T. Welker, J. Lumin., **60**, 275 (994).
[7] T. Igarashi, T. Isobe, M. Sena, Phys. Rev., **B56**, 6444 (1997).
[8] T. Kezuka, M.Konishi, T. Isobe, M.Sena, J. Lumin., **87-89**, 418 (2000).
[9] L. Levi, N. Feltin, D. Ingert, M.P. Pileni, J. Phys. Chem., **B101**, 9153 (1997).
[10] L. Levi, N. Feltin, D. Ingert, M.P. Pileni, J. Cryst. Growth, **184/185**, 377 (1998).
[11] N. Feltin, L.Levi, D. Ingert, M.P. Pileni, J. Phys. Chem., **B103**, 4 (1999).
[12] K. S. Alva, Macromol. Rapid Commun., **17**, 805 (1996).
[13] M. Ikeda, K. Itoh, H. Sato, J.Phys.Soc. Japan, **25**, 455 (1968).
[14] D. S. McClure, J.Chem.Phys., **39**, 2850 (1963).
[15] V. Dimitrova, J.Tate, Thin Solid Films, **365**, 134 (2000).
[16] Shu Man Liu et al., Solid State Commun., **115**, 615 (2000).